PERGAMON

International Journal of Solids and Structures 37 (2000) 7393–7407

INTERNATIONAL JOURNAL OF SOLIDS and STRUCTURES

www.elsevier.com/locate/ijsolstr

Measures of structural damage for global failure analysis

W.B. Krätzig [a], Y.S. Petryna [a,*], F. Stangenberg [b]

[a] *Institute for Statics and Dynamics, Ruhr-University Bochum, Universitätsstr. 150, 44780 Bochum, Germany*

[b] *Institute for Reinforced and Prestressed Concrete Structures, Ruhr-University Bochum, Universitätsstr. 150, 44780 Bochum, Germany*

Received 16 August 1999; in revised form 29 January 2000

Abstract

In building codes, the design of structures is generally based on their virgin state omitting most damage processes and disregarding future physical as well as chemical deterioration. Such concepts of disregard of structural stiffness degradation are in principle incapable of quantifying structural failure and thus of describing important aspects in modern structural engineering.

The present paper supposes the modeling of local damage and deterioration phenomena on material point level and its mapping onto structural level. Here, it demonstrates that global damage measures, i.e. measures on structural level, can stringently be deduced from the reduction of the current structural stiffness, up to now an unsettled problem. Damage indicators are thus observable during incremental-iterative solutions of the tangent stiffness equation, where they estimate the distance from the actual structural state to failure varying from 0 to 1. Their applicability is finally demonstrated exemplarily on a reinforced concrete beam and a large shell.

Keywords: Structural damage; Failure analysis; Damage processes

1. Introduction: Structural damage

In their structural theories, engineers seem to be addicted to the illusion of permanent youth. According to most national standards, structural design concepts are focused on the virgin state of a certain structure and consider neither initial pre-damage nor deterioration nor mechanical damage processes during structural life.

Certainly, some damage processes are well known to engineers and traditionally taken into account, such as limited tension cracking in reinforced concrete structures, high-cycle fatigue or corrosion of steel components, or wear and cracking with crack growth in machinery. All these and many further phenomena will turn a virgin design by materially nonlinear degradation slowly but irresistibly during its lifetime closer and closer to its service termination.

* Corresponding author. Fax: +49-234-709-4149.

E-mail address: y.petryna@sd.ruhr-uni-bochum.de (Y.S. Petryna).

0020-7683/00/$ - see front matter
PII: S0020-7683(00)00204-3

Obviously, each structure, structural element or material point will be sensitive to individual deterioration processes. According to the scale of observation, deterioration phenomena can be studied at all three levels. Micro-mechanical, chemical and biological deteriorations are traditionally described as continuum defects on material point level (Chaboche, 1980; Krajcinovic, 1984). Macro-mechanical descriptions of such phenomena generally use unobservable empirical damage components in the constitutive equations (Carol et al., 1994), even – as in reinforced concrete structures – strongly discontinuous crack damage may develop (Oliver and Simo, 1994). Material deteriorations leading to structural failure are further considered at the element level, such as fatigue or seismic damage of critical cross-sections (Krätzig and Meskouris, 1998). Damage mechanics however since its very beginning (Kachanov, 1958, 1992) is fixed on treatments at material point level. Such modeling of damage in physically nonlinear manner will be pre-supposed in this paper.

Evidently, local concepts of that kind alone disregard principal aspects of structural behavior such as interaction of damage-induced local stress redistribution, load history and global response. Correct global conclusions namely on structural integrity, durability or reliability can be drawn only for the entire structure under the complete spectrum of degradation mechanisms. The attempt of this paper is the description and quantification of such degradation processes on structural level applicable for engineering problems.

2. Nonlinear structural response under damage

Structural damage phenomena are in principle attached to nonlinear responses. All deterioration processes expected to influence a certain structural response behavior have thus to be modeled in numerical simulations in nonlinear manner, particularly in the constitutive laws on material level.

In the present paper, we will presume such suitable classical damage description in the material model. We will then reverse our viewpoint, namely investigating, how to detect and how to identify the arising damage on the global structural level. At this level, in general, structural degradations prejudice the service conditions of the structure and their consequences are externally observable only here.

We start with the most general basic relation for nonlinear structural analysis and consider in Fig. 1 an arbitrary discretized structure, e.g. a shell roof in its deformed state. Further, we assemble in the m-dimensional vector

$$\mathbf{V} = \{V_1, V_2, \ldots, V_i, \ldots, V_m\}$$

all essential nodal degrees of freedom and in

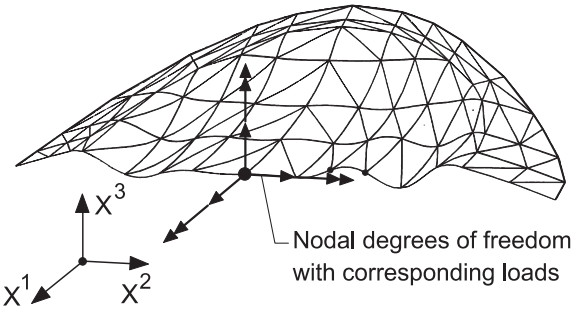

Fig. 1. Discretized structure.

$$\mathbf{P} = \{P_1, P_2, \ldots, P_i, \ldots, P_m\}$$

all corresponding nodal loads. Denoting by $\dot{\mathbf{V}}$, the nodal velocities and $\ddot{\mathbf{V}}$, the nodal accelerations, the nonlinear (differential) equation of motion will have the following form (Krätzig, 1997):

$$\mathbf{M} \cdot \ddot{\mathbf{V}} + \mathbf{G}(\dot{\mathbf{V}}, \mathbf{V}, \mathbf{d}, t) = \mathbf{P}(t). \tag{1}$$

Herein, $\mathbf{M}$ abbreviates the global mass matrix. The nonlinear vector functional $\mathbf{G}$ describes the internal nodal forces due to viscous ($\dot{\mathbf{V}}$) as well as elasto-plastic ($\mathbf{V}$) dynamic equilibrium and due to damage ($\mathbf{d}$). $\mathbf{d}$ represents in most rigorous case an m-dimensional vector of functions describing the structural damage processes on the level of the external variables $\mathbf{V}$, $\mathbf{P}$. In common, technical applications it may degenerate to a set of parameters containing e.g. attained damage accumulations for typical load collectives, or numbers and intensities of single overload events, or just the service life of the structure related to the maintenance intervals. In Eq. (1), t denotes physical time.

We emphasize that the nonlinear equation of motion (1) in general will seldom be known for a realistic nonlinear structural analysis, since the response will be evaluated by incremental-iterative techniques. In order to derive the fundamental equation for such a technique we decompose the external nodal kinematics $\mathbf{V}$, $\dot{\mathbf{V}}$, $\ddot{\mathbf{V}}$, and the external nodal loads $\mathbf{P}$ of a certain unknown (neighboring) structural state is to be determined into those variables $\overline{\mathbf{V}}$, $\overline{\dot{\mathbf{V}}}$, $\overline{\ddot{\mathbf{V}}}$, $\overline{\mathbf{P}}$ of a known fundamental state and increments $\delta\overline{\mathbf{V}}$, $\delta\overline{\dot{\mathbf{V}}}$, $\delta\overline{\ddot{\mathbf{V}}}$, $\delta\overline{\mathbf{P}}$ reaching from it to the neighboring position, e.g.

$$\mathbf{V} = \overline{\mathbf{V}} + \delta\overline{\mathbf{V}}, \qquad \dot{\mathbf{V}} = \overline{\dot{\mathbf{V}}} + \delta\overline{\dot{\mathbf{V}}}, \qquad \ddot{\mathbf{V}} = \overline{\ddot{\mathbf{V}}} + \delta\overline{\ddot{\mathbf{V}}}, \qquad \mathbf{P} = \overline{\mathbf{P}} + \delta\overline{\mathbf{P}}. \tag{2}$$

If we assume all increments as infinitesimally small, we are able to gain from the first variation of Eq. (1) with respect to the kinematic variables of the fundamental state, a linear differential equation for the increments $\delta\overline{\mathbf{V}}$, $\delta\overline{\dot{\mathbf{V}}}$, $\delta\overline{\ddot{\mathbf{V}}}$, namely

$$\mathbf{M} \cdot \delta\overline{\ddot{\mathbf{V}}} + \left.\frac{\partial \mathbf{G}}{\partial \dot{\mathbf{V}}}\right|_{\overline{\dot{\mathbf{V}}}} \cdot \delta\overline{\dot{\mathbf{V}}} + \left.\frac{\partial \mathbf{G}}{\partial \mathbf{V}}\right|_{\overline{\mathbf{V}}} \cdot \delta\overline{\mathbf{V}} = \delta\overline{\mathbf{P}} + \mathbf{R} \tag{3}$$

with the out-of-balance forces of the fundamental state:

$$\overline{\mathbf{R}} = \overline{\mathbf{P}} - \mathbf{M} \cdot \overline{\ddot{\mathbf{V}}} - \mathbf{G}(\overline{\dot{\mathbf{V}}}, \overline{\mathbf{V}}, \mathbf{d}, \mathbf{t}).$$

If we now substitute for the external load $\overline{\mathbf{P}}$ of the fundamental state on the right-hand side of Eq. (3) their counterparts from the left-hand side of the original nonlinear equation of motion (1), we receive the so-called tangent equation of motion

$$\mathbf{M} \cdot \delta\overline{\ddot{\mathbf{V}}} + \mathbf{C}_\mathrm{T} \cdot \delta\overline{\dot{\mathbf{V}}} + \mathbf{K}_\mathrm{T} \cdot \delta\overline{\mathbf{V}} = \mathbf{P} - \mathbf{F}_\mathrm{I} \tag{4}$$

with the following abbreviations:

$\mathbf{C}_\mathrm{T} = \partial\mathbf{G}/\partial\dot{\mathbf{V}}\big|_{\overline{\dot{\mathbf{V}}}}$ – the tangent (viscous) damping matrix,

$\mathbf{K}_\mathrm{T} = \partial\mathbf{G}/\partial\mathbf{V}\big|_{\overline{\mathbf{V}}}$ – the tangent stiffness matrix,

$\mathbf{F}_\mathrm{I} = \mathbf{M} \cdot \overline{\mathbf{V}} - \mathbf{G}(\overline{\mathbf{V}}, \overline{\mathbf{V}}, \mathbf{d}, t)$ – the vector of internal equilibrium nodal forces due to inertia effects, viscous and elasto-plastic as well as deteriorating structural processes for a known fundamental state.

$\mathbf{M}$, $\mathbf{C}_\mathrm{T}$, $\mathbf{K}_\mathrm{T}$ and $\mathbf{F}_\mathrm{I}$ can be evaluated by standard finite element techniques also for material laws containing damage components (Krätzig, 1997). The linearized matrix differential equation (4) is the basis of all nonlinear structural simulations, having for its solution a great number of well-established time-integration algorithms at disposal.

In the following, we will concentrate only on the time-independent variant ($\dot{\mathbf{V}} = \ddot{\mathbf{V}} = \mathbf{0}$) of Eq. (4), an algebraic equation for the determination of $\delta\overline{\mathbf{V}}$, called the tangent stiffness relation:

$$\mathbf{K}_\mathrm{T}(\overline{\mathbf{V}}, \mathbf{d}) \cdot \delta\overline{\mathbf{V}} = \delta\overline{\mathbf{P}} + \overline{\mathbf{R}} = \mathbf{P} - \mathbf{G}(\overline{\mathbf{V}}, \mathbf{d}). \tag{5}$$

For the solution of time-invariant processes by means of Eq. (5) exists a variety of Newton–Raphson-, BFGS- or path-following methods as can be found e.g. in Zienkiewicz and Taylor (1989, 1991) and Bathe (1996).

3. Structural damage simulation

Structural damage is generally understood as a stiffness softening phenomenon caused by material deterioration. Softening of a nonlinear structural response is mirrored in the corresponding load–displacement diagram $\mathbf{P} = \mathbf{P}(\mathbf{V})$ by a change of its slope, more precisely between loading and unloading for different load cycles. So obviously, all damaging effects of a certain response must be stored in the vector functional $\mathbf{G}(\dot{\mathbf{V}}, \mathbf{V}, \mathbf{d}, t)$ of Eq. (1), and because of the definition of $\mathbf{K}_T$ following Eq. (4) also in the tangent stiffness matrix. For unloading paths, the tangent stiffness corresponds evidently with the secant stiffness. In order to distinguish stiffness softening due to elasto plastic or large elastic deformations from damage-caused weakening, $\mathbf{K}_T$ and $\mathbf{G}$ must change in dependence of the vectorial damage variable $\mathbf{d}$:

$$\frac{\partial \mathbf{G}}{\partial \mathbf{d}} \neq 0 \quad \text{and} \quad \frac{\partial \mathbf{K}_T}{\partial \mathbf{d}} \neq 0. \tag{6}$$

If modifications of $\mathbf{G}$ and $\mathbf{K}_T$ (6) caused by degradations occur, a nonlinear damage process arises. Driven by the deterioration process, the structural response behavior will change over lifetime generally in nonlinear manner. Thus, the damage accumulation will be nonlinear, and any computer simulation of the response must also be nonlinear. Consequently, the tangent stiffness relation (5) or the tangent equation of motion (4) has to be integrated over lifetime intervals with successively changing stiffness properties.

Here we will omit all further approximations for technical applications, where damage processes often are assumed as so local that their effects on the tangent stiffness matrix $\mathbf{K}_T$ and on the internal nodal force vector $\mathbf{G}$ can be ignored. If in addition to this neglect all inelastic material properties are suppressed

$$\begin{aligned} &\frac{\partial \mathbf{G}}{\partial \mathbf{d}} = \mathbf{0}, \qquad \frac{\partial \mathbf{K}_T}{\partial \mathbf{d}} = \mathbf{0}, \\ &\mathbf{G}(\mathbf{V}, \mathbf{d}) \approx \mathbf{G}_{el}, \qquad \mathbf{K}_T(\mathbf{V}, \mathbf{d}) \approx \mathbf{K}_{el}, \end{aligned} \tag{7}$$

then the completely linearized tangent stiffness relation forms an algorithm for the original total variables $\mathbf{V}$, $\mathbf{P}$ (2)

$$\mathbf{K}_T \cdot \delta\overline{\mathbf{V}} = \delta\overline{\mathbf{P}} \;\rightarrow\; \mathbf{K}_{el} \cdot \mathbf{V} = \mathbf{P} \tag{8}$$

solvable in one step separating the damaged "weak links" completely from the response of the entire structure. The index *el* characterizes linear elastic variables.

Classical high-cycle fatigue and most crack-propagation problems are encountered by such approximate linearized concepts, in which all stresses are evaluated for the non-damaged elastic structure (Yao et al., 1986).

Focusing now again on nonlinear (real) deterioration processes, we conclude that all available information on structural damage has to be provided in the constitutive relations and is transferred from there into the tangent stiffness matrix $\mathbf{K}_T$. The numerical techniques for this damage aggregation in $\mathbf{K}_T$ are the so-called multi-level or multi-scale simulation concepts (Krätzig, 1997). In this solution process of Eq. (8), $\mathbf{K}_T$ is calculated regularly at each load step, such that the question is raised: How to extract this information from $\mathbf{K}_T$?

4. Damage indicators and measures of structural integrity

For this objective, we return to a discretized structure with m degrees of freedom V_i, $1 \leqslant i \leqslant m$. The structure shall be subjected to external loads $\mathbf{P}$ and to deterioration phenomena $\mathbf{d}$ leading to a damage process observable in $\mathbf{K}_T$. For convenience, the tangent stiffness matrix $\mathbf{K}_T$, a $(m \times m)$ square matrix is assumed to be symmetric and positively definite (Bazant and Cedolin, 1991), if we exclude structural instabilities. In $\mathbf{K}_T$ are stored $(m^2 + m)/2$ different real, scalar-valued element informations, characteristic for the damage process. Their most condensed form are the m real, positive eigenvalues of $\mathbf{K}_T$ from which damage indicators can be derived.

A damage indicator D_i for a certain state of deformation $\mathbf{V}$ should take the value 0 in the undamaged, virgin state $\mathbf{d} = 0$ and increase with growing damage. Further, just in case of structural disintegration, D_i should arrive at the value 1. Of course, in technical reality such critical damage barriers will seldom be reached. It should be mentioned that existing damage indicators are in most cases problem-dependent (Yao et al., 1986) or related to sectional level (see e.g. the survey in Krätzig and Meskouris (1998)) and will seldom follow this clear systematics. Such a set D_i of generalized and normalized damage indicators can be appropriately defined by

$$D_i(\mathbf{V}, \mathbf{d}) = \frac{\lambda_i^*(\mathbf{V}_0, \mathbf{d} = \mathbf{0}) - \lambda_i^*(\mathbf{V}, \mathbf{d})}{\lambda_i^*(\mathbf{V}_0, \mathbf{d} = \mathbf{0})} = 1 - \frac{\lambda_i^*(\mathbf{V}, \mathbf{d})}{\lambda_i^*(\mathbf{V}_0, \mathbf{d} = \mathbf{0})}, \tag{9}$$

which obviously performs the above-mentioned requirements. The second term herein, the deviation from 1, describes as measure of structural integrity the normalized distance of the structure from the point of failure.

For the λ_i^*, a number of different functions derived from $\mathbf{K}_T$ can be selected:

(1) Eigenvalues of $\mathbf{K}_T(\mathbf{V}, \mathbf{d})$ as principal stiffness parameters.

The eigenvalue spectrum λ_i, $1 \leqslant i \leqslant m$ of $\mathbf{K}_T$

$$\lambda_1(\mathbf{V}, \mathbf{d}), \lambda_2(\mathbf{V}, \mathbf{d}), \ldots, \lambda_i(\mathbf{V}, \mathbf{d}), \ldots, \lambda_m(\mathbf{V}, \mathbf{d}) \tag{10}$$

forms a set of real positive scalars, which are as principal stiffnesses an optimal basis for definition of damage indicators (9). In the sequel, we will concentrate solely on the set D_i (9) based on evolutions of λ_i (or ω_i^2) as representations of the damaged state of the structure. The interesting aspect of mode conversion of corresponding mode shapes $\mathbf{\Phi}_i$ (or $\mathbf{\Phi}_i^*$) during the damage process shall only be mentioned briefly. Obviously, one gets at least a qualitative impression of the degraded configuration by the set of corresponding eigenmodes of $\mathbf{K}_T$, as Fig. 2 demonstrates. Here, the first eigenform of a virgin cooling tower shell (left) is compared with the first eigenform of a wind-damaged one under deadweight and 1.4 of design wind load. Finally, and for the next viewpoint, we recall that the eigenvalues λ_i and the eigenforms $\mathbf{\Phi}_i$ stem from a mapping process of $\mathbf{K}_T$ on a $(m \times m)$ unit matrix $\mathbf{I}$

$$(\mathbf{K}_T(\mathbf{V}, \mathbf{d}) - \lambda_i \mathbf{I})\mathbf{\Phi}_i = 0. \tag{11}$$

(2) Structural eigenfrequencies ω_i, $1 \leqslant i \leqslant m$ of $\mathbf{K}_T(\mathbf{V}, \mathbf{d})$ and $\mathbf{M}$.

Disadvantageously only few finite element codes provide eigenvalue solvers, but most of them contain software for eigenfrequency analysis. Obviously, its basic generalized eigenvalue problem

$$\left(\mathbf{K}_T(\mathbf{V}, \mathbf{d}) - \omega_i^2 \mathbf{M}\right)\mathbf{\Phi}_i^* = 0 \tag{12}$$

describes a mapping of $\mathbf{K}_T$ on the global mass matrix $\mathbf{M}$ of the structure, and unless the mass is not distributed too unevenly over the system, (12) will give qualitatively very similar results compared to Eq. (11). Also the natural vibration mode shapes $\mathbf{\Phi}_i^*$, corresponding to eigenfrequencies ω_i^2, give very similar impressions of the influence of damage processes on the deformation property of a structure, as $\mathbf{\Phi}_i$ do.

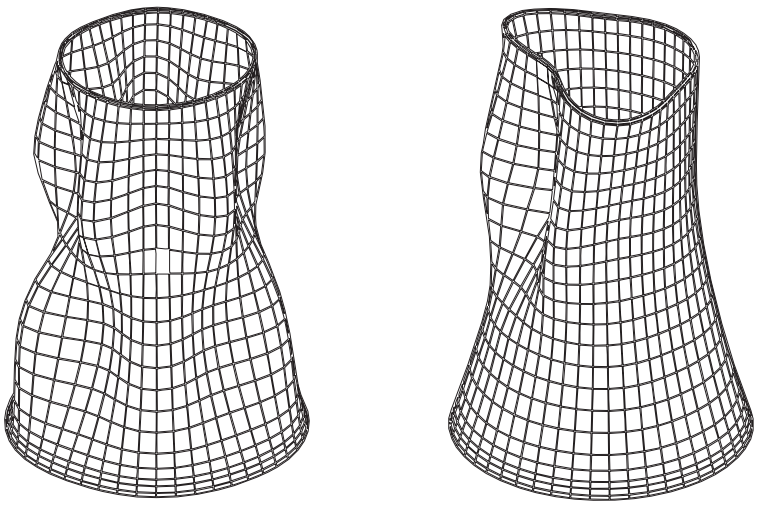

Fig. 2. First mode shapes of a virgin (left) and wind-damaged (right) cooling tower shell.

Recently, instead of eigenvalues of $\mathbf{K}_{\mathrm{T}}$, the use of their singular values has been proposed (Lenzen and Waller, 1997), combined with the so-called dynamic influence functions: For a symmetric, positive definite matrix as $\mathbf{K}_{\mathrm{T}}$, singular values are the squares of eigenvalues.

Obviously, a strong pre-supposition for structural integrity is the non-singularity and positive definiteness of $\mathbf{K}_{\mathrm{T}}$, which renders all eigenvalues real and positive:

$$\det \mathbf{K}_{\mathrm{T}} > 0, \qquad \delta\mathbf{V}^{\mathrm{T}} \cdot \mathbf{K}_{\mathrm{T}} \cdot \delta\mathbf{V} > 0 : \forall \lambda_i > 0 \\ \forall D_i(\mathbf{V}, \mathbf{d}) < 1, \;\; 1 \leqslant i \leqslant m. \tag{13}$$

Thus, the transition from structural integrity to disintegration is initiated by the first zero eigenvalue of $\mathbf{K}_{\mathrm{T}}$

$$\det \mathbf{K}_{\mathrm{T}} = 0, \qquad \delta\mathbf{V}^{\mathrm{T}} \cdot \mathbf{K}_{\mathrm{T}} \cdot \delta\mathbf{V} \geqslant 0 : \forall \lambda_i \geqslant 0, \;\; \exists \lambda_i = 0 \\ \forall D_i(\mathbf{V}, \mathbf{d}) \leqslant 1, \;\; \exists D_i(\mathbf{V}, \mathbf{d}) = 1. \tag{14}$$

With one $\lambda_i = 0$, a transition from structural integrity to loss of integrity via a single-fold damage-mode transition $\mathbf{\Phi}_L$ will start, multiple $\lambda_i = 0$ deliver a multiple damage-mode transition, and all $\lambda_i = 0$ finally lead to a complete disintegration. In the case of a single $\lambda_i = 0$, the degree of structural loss of integrity is $g = 1$. For multiple zero eigenvalues or even for negative ones, higher degrees of loss of integrity may (theoretically) appear:

$$g = r + r^* = \mathrm{num}(\lambda_i = 0) + \mathrm{num}(\lambda_i < 0). \tag{15}$$

These recognitions are formally identical to time-independent structural instabilities. But one should observe one important difference: bifurcation modes e.g. form an ambiguous path offer to the structure, which it may accept or not, while a damage mode is always a constraint path.

Obviously zero eigenvalues of $\mathbf{K}_{\mathrm{T}}$ decide on the transition from structural integrity to disintegration. If only these transition points are of special interest, one can find them from the central diagonal matrix $\mathbf{K}_{\mathrm{T}D}$ of the Cholesky-decomposition of $\mathbf{K}_{\mathrm{T}}$. In this concept, the tangent matrix is decomposed

$$\mathbf{K}_{\mathrm{T}} = \mathbf{K}_{\mathrm{T}}^{*\mathrm{T}} \cdot \mathbf{K}_{\mathrm{T}D} \cdot \mathbf{K}_{\mathrm{T}}^{*} \tag{16}$$

into the upper triangular matrix $\mathbf{K}_{\mathrm{T}}^{*}$ with unit values on the main diagonal and the pure diagonal matrix $\mathbf{K}_{\mathrm{T}D}$. In the solution procedure of Eq. (5) their diagonal terms $k_{D1}, k_{D2}, \ldots, k_{Di}, \ldots, k_{Dm}$ are generally stored

in the computer and thus available to the user. They mirror certain properties of the eigenvalues of $\mathbf{K}_T$ (Zurmühl and Falck, 1984) such as

$$\det \mathbf{K}_T = \lambda_1 \cdot \lambda_2 \cdot \cdots \lambda_i \cdot \cdots \cdot \lambda_m = k_{D1} \cdot k_{D2} \cdot \cdots \cdot k_{Di} \cdot \cdots \cdot k_{Dm}. \tag{17}$$

Clearly, diagonal elements of $\mathbf{K}_{TD}$ are not identical with the eigenvalues of $\mathbf{K}_T$, but contain all properties of them with respect to $\det \mathbf{K}_T$. Also other related approaches based on decomposition of $\mathbf{K}_T$ may certainly be applied, as it has been done in Section 6.1.

5. Applied degradation models

The deterioration phenomena considered in the later failure simulations of reinforced concrete structures shall be briefly explained in this section. Usually in failure analysis the so-called load-induced and time-dependent deteriorations are distinguished. Load-induced deteriorations are usually interpreted as irreversible material damage effects, presumably incorporated into the material models of suitable finite element software. These are for example (Krätzig and Zahlten, 1989),

- nonlinear cyclic stress–strain behavior of concrete in compression;
- monotonic and recursive tension cracking of concrete;
- elasto-plastic behavior of the reinforcement steel;
- inelastic bond behavior.

Corresponding changes of the material state and their influence on the stiffness parameters may be illustrated on the uniaxial material diagram for reinforced concrete in Fig. 3. For instance, concrete tension cracking leads to replacement of the effective elasticity modulus E_c^{eff} (concrete + steel) by that one of steel alone E_s^0 passing through the bond effects modeled by tension stiffening/softening. Yielding of reinforcement leads to replacement of the initial elasticity modulus E_s^0 by its reduced counterpart E_s^T. Inelastic compressive behavior of concrete is characterized by a permanent change of its current elasticity modulus E_c.

Among various time-dependent deterioration phenomena, we consider in this contribution representatively steel corrosion according to Sarja and Vesikari (1996). This model is characterized by the initiation time t_0 and the corrosion rate k_s. The reduction of the steel cross-section A_s after initiation of corrosion (Fig. 4) is modeled as follows:

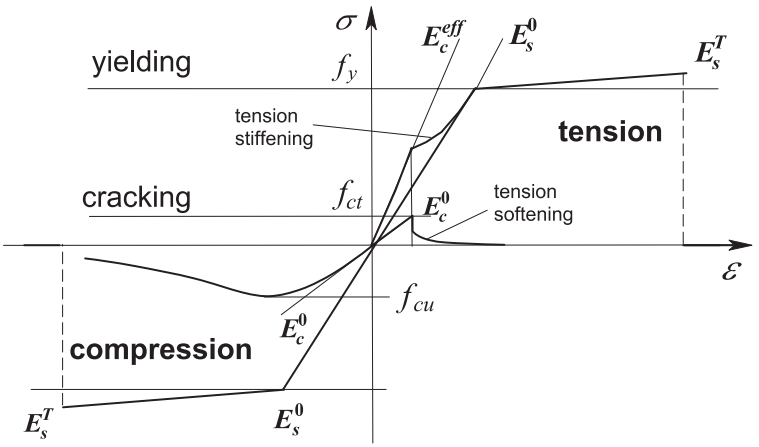

Fig. 3. Uniaxial stress–strain diagram for reinforced concrete.

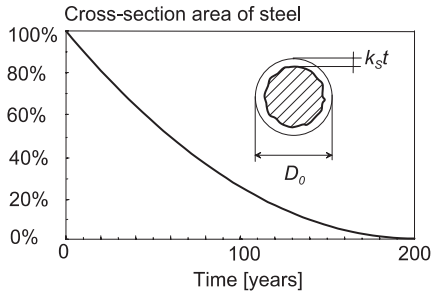

Fig. 4. Corrosion of reinforcement.

$$A_s(t) = N\frac{\pi(D_0 - k_s t)^2}{4}, \tag{18}$$

where N denotes the number of reinforcement bars, D_0 their initial diameter, k_s the corrosion rate and t the corrosion time. The reduced amount of reinforcement due to corrosion (18) will evidently cause a decrease of structural stiffness especially in the cracked elements, where the role of reinforcement is dominant.

These material deterioration effects are directly incorporated into the code for the evaluation of the element matrices and thus automatically assembled in the global stiffness matrix $\mathbf{K}_T$ of the structure. This integral information on structural damage can then be extracted from $\mathbf{K}_T$ and in this way quantified in the global damage indicators (9).

6. Numerical example

6.1. Damage description

Applying consequently the above presented approach, we now derive local damage indicators from Eq. (9). However, instead of eigenvalues (10) of $\mathbf{K}_T$, the diagonal values $a_i^u = a_{ii}^u$ of the upper triangular matrix $\mathbf{K}_T^u$ of the Gauss elimination procedure

$$\mathbf{K}_T^u = \mathbf{T} \cdot \mathbf{K}_T = \{a_{ij}^u\} = \begin{cases} = 0 : i > j \\ \neq 0 : i \leqslant j \end{cases} \tag{19}$$

offers a further alternative to λ_i^* (9). In Eq. (19) $\mathbf{T}$ denotes the corresponding transformation matrix. Evidently (Zurmühl and Falck, 1984), in a_i^u the original deterioration properties of $\mathbf{K}_T$ are preserved.

The advantage of the use of a_i^u lies in the fact that no additional calculations are required to obtain them. They are all automatically available at each step of the solution process of Eq. (5).

Then, the set of damage indicators D_i can be evaluated applying these diagonal values according to Eq. (9):

$$D_i(\mathbf{V}, \mathbf{d}) = 1 - \frac{a_i^u(\mathbf{V}, \mathbf{d})}{a_i^u(\mathbf{V}_0, \mathbf{d} = \mathbf{0})} \tag{20}$$

forming the basis for further damage estimates.

How can one practically work with structural damage indicators D_i, a set of m time- or load-dependent functions? In order to condense the available information for monotonic loading processes, an integrated global damage measure as maximum value of the individual damage indicators (20) is

$$D_{\max} = \max\{D_i\}, \quad i = 1, \ldots, N, \tag{21}$$

which ranges from 0 in the nondamaged state to exactly 1 in case of global failure, since then the stiffness matrix $\mathbf{K}_T$ becomes singular and at least one of its eigenvalues will be zero. If instability problems are eliminated, for instance by subtraction of the geometrical stiffness matrix $\mathbf{K}_G$ from $\mathbf{K}_T$

$$\mathbf{K}_D = \mathbf{K}_T - \mathbf{K}_G, \tag{22}$$

then this singularity describes purely the loss of structural capacity due to physical damage by unlimited displacements up to collapse. In that sense D_{max} reflects the maximum accumulated damage or the loss of capacity, while its distance to 1, the maximum measure of structural integrity (9)

$$R = 1 - D_{max} \tag{23}$$

displays the residual capacity up to global failure.

Besides Eq. (21), other integral measures for the estimation of structural damage based on the local damage indicators (9) and (20) can be defined. Accumulated damage due to cyclic loading can be well described by the following weighted arithmetic mean value:

$$D_{wam} = \frac{\sum D_i^2}{\sum D_i}, \tag{24}$$

which includes all individual damage contributions emphasizing the significant values.

6.2. Reinforced concrete beam

For numerical illustration, a simply supported RC beam with two spans of 10.00 m under uniformly distributed vertical operation load has been chosen (Fig. 5). Its required material parameters are given in Table 1. The beam is modeled as a layered continuum consisting of two uniaxial steel layers on both faces, and of 12 plane-stress concrete layers.

Each concrete (and steel) layer is mapped on an isoparametric four node Reissner–Mindlin shell element capable for large displacements and large rotations. Thickness changes are not considered. The displacement shape functions of the element are bilinear polynomials, and to avoid transverse shear locking the internal shear deformations are linearly interpolated in the sense of an assumed strain element. This element is also able to model "narow" plates like beams.

A multi-level simulation concept (Krätzig, 1997) has been applied to solve the tangent stiffness equation

$$\overset{+}{\mathbf{V}} = (\mathbf{K}_T(\mathbf{V}, \mathbf{d}))^{-1} \cdot (\mathbf{P} - \mathbf{F}_i(\mathbf{V}, \mathbf{d})) \tag{25}$$

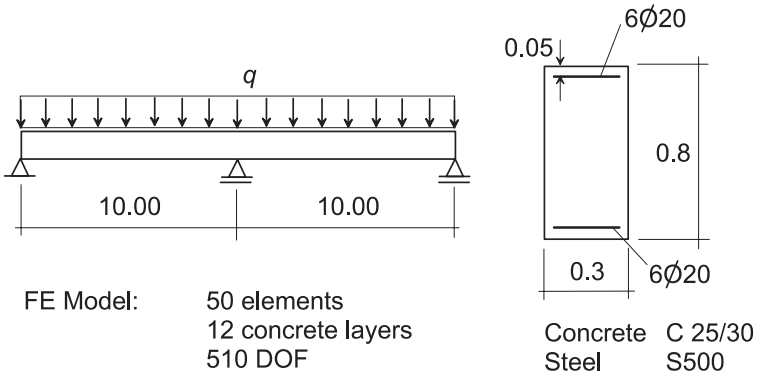

Fig. 5. Reinforced concrete beam under operation load q.

Table 1
Material parameters

Concrete C25/30	
f_{cm}	33 MN/m^2
f_{ctm}	2.6 MN/m^2
E_{cm}	30 500 MN/m^2
Steel S500	
f_{ym}	550 MN/m^2
f_{tm}	594 MN/m^2
E_s	200 000 MN/m^2

for this layered discretized model in incremental-iterative manner. The analysis has been carried out within the FEMAS-software developed at the Ruhr-University Bochum (Beem et al., 1996).

The deformation process of the beam under quasi-statically increased loading is depicted by the response curve in Fig. 6 for both mid-span points. It is characterized first by tension cracking, then by yielding of reinforcement at the central support as well as in both spans, and finally by collapse under $q = 78$ kN/m initiated by concrete compression failure over the central support.

Simultaneously, the global damage indicator D_{max} has been monitored at each step of the loading process. As can be seen from its evolution in Fig. 7, the damage indicator responds rather sensitive with jumps to every new damage observed. The first one (above point 1) corresponds to tension cracking over the central support, the second one (point 2) to cracking in both spans. Further, load increase leads to a monotonic damage accumulation through crack propagation over the beam length and height. Further, yielding of reinforcement over the central support (point 3) causes increase of its value up to 0.9 as a warning of the almost exhausted capacity reserves. When the same happens in both spans (point 4), the last increase of D_{max} to 0.98 predicts the succeeding collapse.

In order to estimate accumulated damages under cyclic loads, the beam has been charged quasi-statically 10 times up to $q = 64$ kN/m each time followed by a complete unloading. At this load level both concrete cracking and reinforcement yielding took place. The nonlinear character of the damage accumulation can clearly be observed in Fig. 8 by means of the weighted mean value D_{wam}. Damage propagation over the beam occurs with increasing intensities, demonstrating a typical progressive damage process.

Finally, for the evolution of the beam response under corroded reinforcement, corrosion has been taken into account with the rate $k_s = 0.004$ cm/year (Sarja and Vesikari, 1996) resulting in a relative reduction of the steel cross-section of 35% in 100 years (Table 2). One can easily observe the corresponding reduction of carrying capacity from the response curves in Fig. 9 calculated for 0, 20, 40, 60 and 80 years of corrosion life

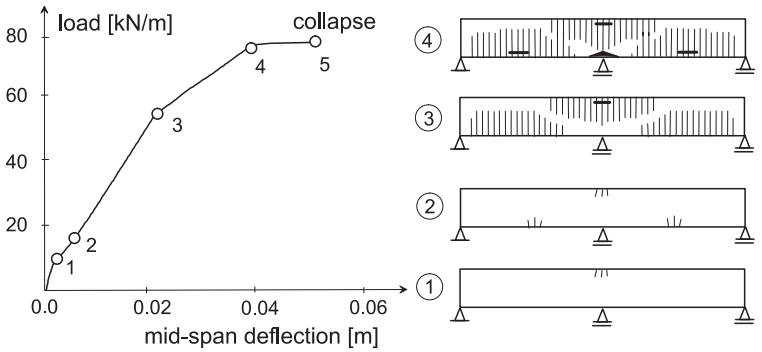

Fig. 6. Beam response under quasi-static loading.

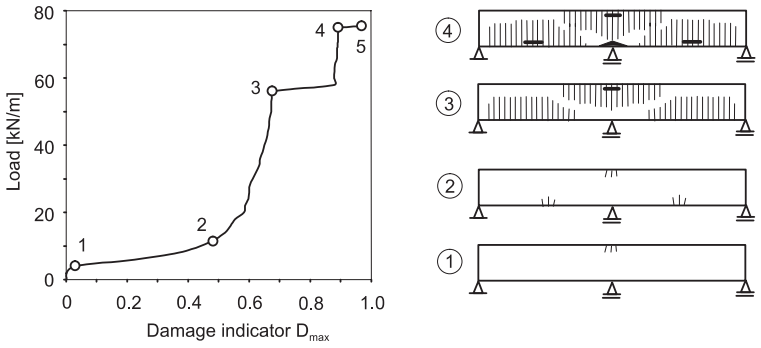

Fig. 7. Damage measure for monotonic loading.

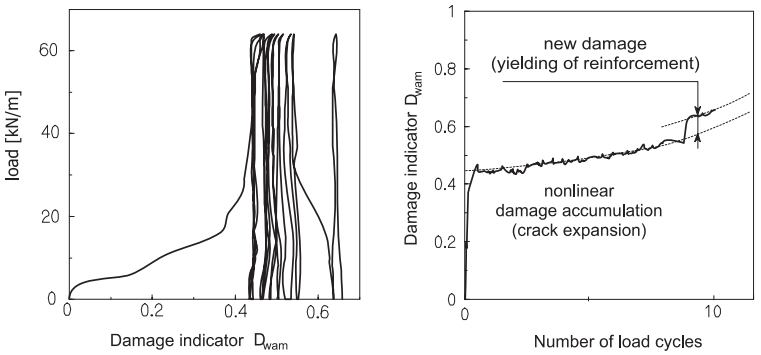

Fig. 8. Damage measure for cyclic loading.

Table 2
Beam response under corrosion

Time, t (years)	Steel cross-section, A_s (cm^2)	Carrying capacity, q_c (kN/m)	Damage indicator, D_{max}, by $q_d = 43$ kN/m
0	18.85	78.0	0.682
20	17.30	72.0	0.700
40	15.95	66.0	0.718
60	14.59	60.0	0.901
80	13.30	54.5	0.915

or from Table 2. Here, the damage indicator D_{max} has been evaluated for each corrosion time instant under design load $q_d = 43$ kN/m demonstrating a significant jump from 0.73 to 0.91 between 60 and 80 years of corrosion.

6.3. Cooling tower shell

As a second example, damage evolution shall now be demonstrated by the example of a large cooling tower shell. Fig. 10 shows this shell of revolution with its varying wall thickness over the height. The tower will be subjected to its dead weight G, a quasi-static wind load W, and service temperature effects ΔT. The

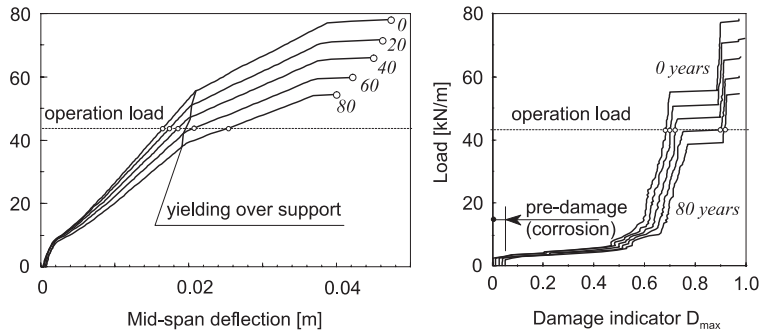

Fig. 9. Damage evaluation under corrosion.

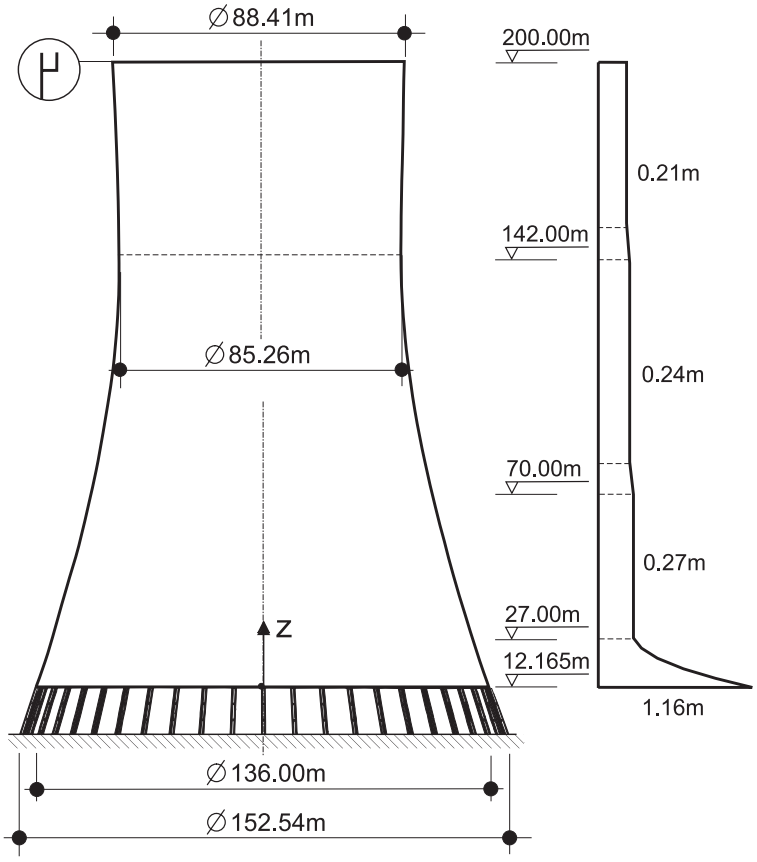

Fig. 10. Natural draft cooling tower shell.

wind load will be increased by a load-factor λ reaching from zero up to collapse. The complete data of the shell and its response behavior can be found in the work of Krätzig and Noh (1998).

The cooling tower shell again is modeled as a layered reinforced concrete continuum consisting of steel layers, uniaxial and orthogonal to each other on both faces, and of plane-stress concrete layers, which

material properties mentioned earlier. The complete discretization process and the failure analysis is described by Krätzig et al. (1998).

Fig. 11 offers plots of the first three damage indicators (9) based on the eigenfrequencies ω_1, ω_2 and ω_3 of this cooling tower shell, demonstrating the steep damage evolution in the structure after $\lambda \approx 1.3$, the onset of wide-spread cracking. Of interest in this connection is the corresponding damage curve for dead weight G and increasing wind load λW at winter service conditions with a temperature difference from outside to inside air of $\Delta T = 45$ K on Fig. 12. Obviously, the cooling tower shell in this case is already for zero wind

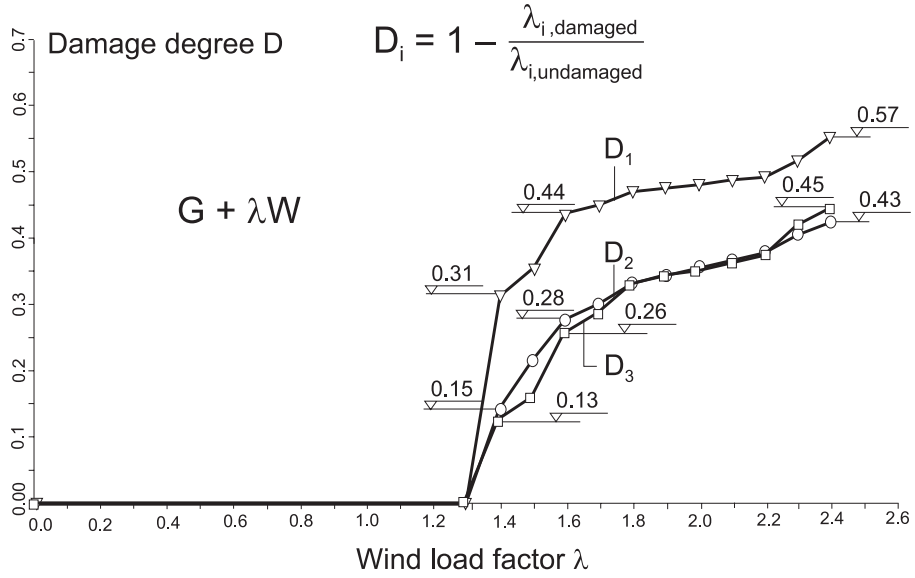

Fig. 11. Damage evolution under dead load and wind.

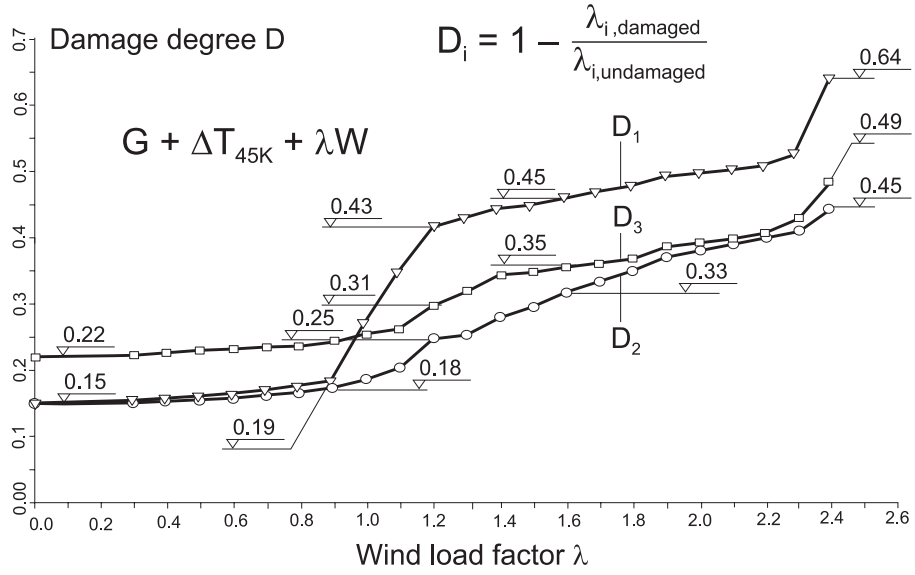

Fig. 12. Damage evolution under dead load, wind and winter temperature conditions.

speeds in a considerable state of damage $D_{\max} = 0.22$. For high wind velocities, the damage remains in the same order of magnitude than for out-of-service conditions ($\Delta T = 0$), a well-known phenomenon to reinforced concrete designers: As soon as cracking appears, temperature effects become subordinate.

7. Conclusions

During their service lives engineering structures are subjected to various technical and environmental actions causing damage processes and leading finally to structural failure. This engineering reality however is still not properly reflected in engineering design concepts due to lack of theory and experience with structural damage. On the other hand, substantial knowledge has been accumulated in recent decades in computational damage mechanics on material level. The present paper bridges both fields in order to form the basis for urgent progress in structural damage analysis.

Since usually incremental tangent operators are at disposal for the solution of nonlinear problems, the tangent stiffness matrix may serve as a natural source of damage information on structural level. The paper, thus, proposes damage measures evaluated from the evolution of the global tangent stiffness matrix $\mathbf{K}_T$, and demonstrates their applicability to different types of damage-oriented structural failure analysis. Thus, it presents the first steps in developing a general structural damage concept, and it may stimulate much further work in this direction.

Acknowledgements

Financial support of the DFG (German Science Foundation) within the Special Research Center 398 at the Ruhr-University Bochum and of the European Union under Copernicus, Contract-No. ERBIC 15CT96 O755 is gratefully acknowledged.

References

Bathe, K.-J., 1996. The Finite Element Procedures. Prentice Hall, New Jersey.

Bazant, Z., Cedolin, L., 1991. Stability of Structures. Oxford University Press, New York.

Beem, H., Könke, C., Montag, U., Zahlten, W., 1996. FEMAS-2000 – Users Manual. Release 3.0. Institute for Statics and Dynamics, Ruhr-University Bochum, Germany.

Carol, I., Rizzi, E., Willam, K., 1994. Towards a general formulation of elastic degradation and damage based on a loading surface. In: Mang, H., Bicanic, N., de Borst, R. (Eds.), EURO-C, Cromwell Press Ltd, Melksham, UK, pp. 199–208.

Chaboche, J., 1980. Continuum damage mechanics. Part I and II. ASME Journal of Applied Mechanics 55, 59–72.

Kachanov, L., 1992. Introduction to continuum damage mechanics. Boston, Martinus Nijhof.

Kachanov, M., 1958. On the time to failure under creep conditions. Izv. Acad. Nauk SSSR Otd. Tekhn. Nauk 8, 26–31.

Krajcinovic, D., 1984. Continuum damage mechanics. Applied Mechanics Reviews 37 (1), 1–6.

Krätzig, W.B., 1997. Multi-level modeling techniques for elasto-plastic structural responses. In: Owen, D., Oñate, E., Hinton, E. (Eds.), Computational Plasticity, Proceedings of Fifth International Conference, Part 1, CIMNE – Int. Center for Num. Meth. in Engng., Barcelona, Spain, pp. 457–468.

Krätzig, W.B., Könke, C., Mancevski, D., Gruber, K.P., 1998. Design for durability of natural draught cooling towers by life-cycle simulations. Engineering Structures 20 (10), 899–908.

Krätzig, W.B., Meskouris, K., 1998. Assessment of seismic structural vulnerability as a low-cycle-fatigue process. In : Bisch, P., Labb, P., Pecker, A. (Eds.), Proceedings of the 11th European Conference on Earthquake Engineering, Invited Lectures, Paris, A.A. Balkema, Rotterdam, 1998, p. 440–457.

Krätzig, W.B., Noh, S.-Y., 1998. On nonlinear-progressive damage processes of structures. Bauingenieur 73 (6), 273–276.

Krätzig, W.B., Zahlten, W., 1989. The application of plastic fracturing theory to the finite element analysis of general reinforced shells. In: 10th International Conference on Structural Mechanics in Reactor Technology, vol. B, SMIRT X, Anaheim, USA, 1989, pp. 311–322.

Lenzen, A., Waller, H., 1997. Identification using the algorithm of singular value decomposition. Mechanical Systems and Signal Processing 11, 441–457.

Oliver, J., Simo, J., 1994. Modelling strong discontinuities by means of strain softening constitutive equations. In: Mang, H., Bicanic, N., de Borst, R. (Eds.), EURO-C, Cromwell Press, Melksham, UK, pp. 363–372.

Sarja, A., Vesikari, E. (Eds.), 1996. Durability design of concrete structures. Report of RILEM Technical Committee 130-CSL. E & FN Spon, London.

Yao, J.T.P., Kozin, F., Wen, Y.-K., Yang, J.-N., Schueller, G.I., Ditlevsen, O., 1986. Stochastic fatigue, fracture and damage analysis. Structural Safety 3, 231–267.

Zienkiewicz, O., Taylor, R., 1989. The Finite Element Method. vol. 1, McGraw-Hill, London.

Zienkiewicz, O., Taylor, R., 1991. The Finite Element Method. vol. 2, McGraw-Hill, London.

Zurmühl, R., Falck, S., Matrizen und ihre Anwendungen für Mathematiker, Physiker und Ingenieure. Teil 1, 2. 5. Auflage, Springer, Berlin.